

Supplementary Material

Biological luminescent metal-organic framework with high fluorescence quantum yield for the selective detection of amino acids and monosaccharides

Ying-Ying Zhou^a, Yuan Xu^a, Maoxing Yu^b, Yi Xiong^b, Xun-Gao Liu^{a,*}, Zujin Zhao^{b,*}

^a College of Material, Chemistry and Chemical Engineering, Hangzhou Normal University, Hangzhou, 310036, China

^b State Key Laboratory of Luminescent Materials and Devices, Guangdong Provincial Key Laboratory of Luminescence from Molecular Aggregates, South China University of Technology, Guangzhou, 510640, China

*Corresponding author: xungaoliu@hznu.edu.cn (X.-G. Liu); mszjzhao@scut.edu.cn (Z. Zhao).

Table S1. Crystal data and structure refinements for complex **1**

Compound	Complex 1
Formula	C ₂₆₄ H ₁₉₂ N ₄₄ O ₃₄ Zn ₁₂
<i>M</i>	5309.29
crystal system	orthorhombic
space group	Ccca
<i>a</i> /Å	9.9878(11)
<i>b</i> /Å	42.445(5)
<i>c</i> /Å	42.607(4)
<i>α</i> /deg	90
<i>β</i> /deg	90
<i>γ</i> /deg	90
<i>V</i> /Å ³	18063(3)
<i>Z</i>	2
temperature/K	150
<i>λ</i> (radiation wavelength)/Å	0.71073
<i>D</i> (g/cm ³)	0.976
reflections collected	71109
<i>R</i> ₁ ^a [<i>I</i> > 2σ(<i>I</i>)]	0.0287
<i>wR</i> ₂ ^b [<i>I</i> > 2σ(<i>I</i>)]	0.0640
goodness-of-fit	1.055
CCDC no.	2071053

$${}^aR_1 = \sum |F_o - F_c| / \sum |F_o|, \quad {}^b wR_2 = [\sum [w(F_o^2 - F_c^2)^2] / \sum w(F_o^2)^2]^{1/2}$$

Table S2. Selected bond lengths (Å) and angles (°) for complex **1**.

Zn(1)-O(1A)	1.9115(2)	Zn(2)-O(3)	2.7010(2)
Zn(1)-O(1B)	1.9115(2)	Zn(2)-O(4)	1.9531(1)
Zn(1)-N(2C)	2.0176(1)	Zn(2)-O(5)	1.9819(1)
Zn(1)-N(2D)	2.0176(1)	Zn(2)-N(1)	1.9699(1)
		Zn(2)-N(4)	2.0577(1)
O(1A)-Zn(1)-O(1B)	126.538(11)	O(3)-Zn(2)-O(4)	53.377(6)
O(1A)-Zn(1)-N(2C)	102.719(7)	O(3)-Zn(2)-O(5)	162.700(7)
O(1A)-Zn(1)-N(2D)	112.277(8)	O(3)-Zn(2)-N(1)	86.116(8)
O(1B)-Zn(1)-N(2C)	112.277(8)	O(3)-Zn(2)-N(4)	86.381(6)
O(1B)-Zn(1)-N(2D)	102.719(7)	O(4)-Zn(2)-O(5)	109.372(9)
N(2C)-Zn(1)-N(2D)	96.462(6)	O(4)-Zn(2)-N(1)	113.730(8)
		O(4)-Zn(2)-N(4)	119.328(6)
		O(5)-Zn(2)-N(1)	101.991(6)
		O(5)-Zn(2)-N(4)	105.873(6)
		N(1)-Zn(2)-N(4)	104.916(7)

A: $1-x, 0.5+y, 0.5+z$; B: $1+x, 1-y, 0.5+z$ C: $2-x, y, 1.5-z$ D: $x, 1.5-y, 1.5-z$

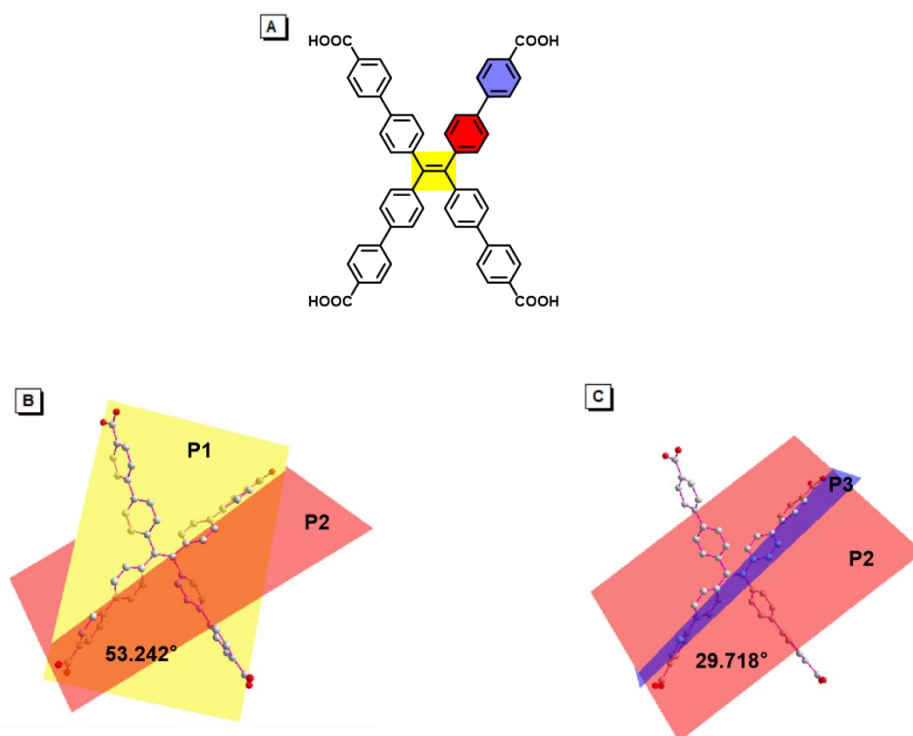


Fig. S1. (A) The plane of the two C atoms forming central C=C double bond and four C atoms surround them is named P1. The planes crossing phenyl rings attached C=C double bond are named P2. The planes of phenyl rings connected with carboxylic groups are named P3. The average dihedral angles are labeled for (B) P1-P2 and (C) P2-P3 in complex **1**.

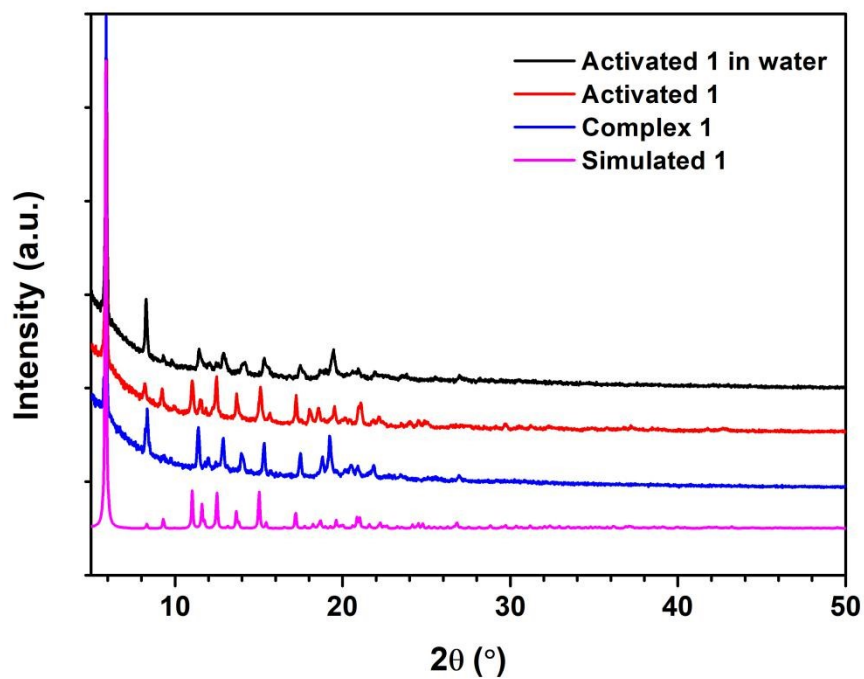


Fig. S2. The PXRD patterns of simulated **1** (magenta), complex **1** (blue), activated **1** (red) and activated **1** in water (black).

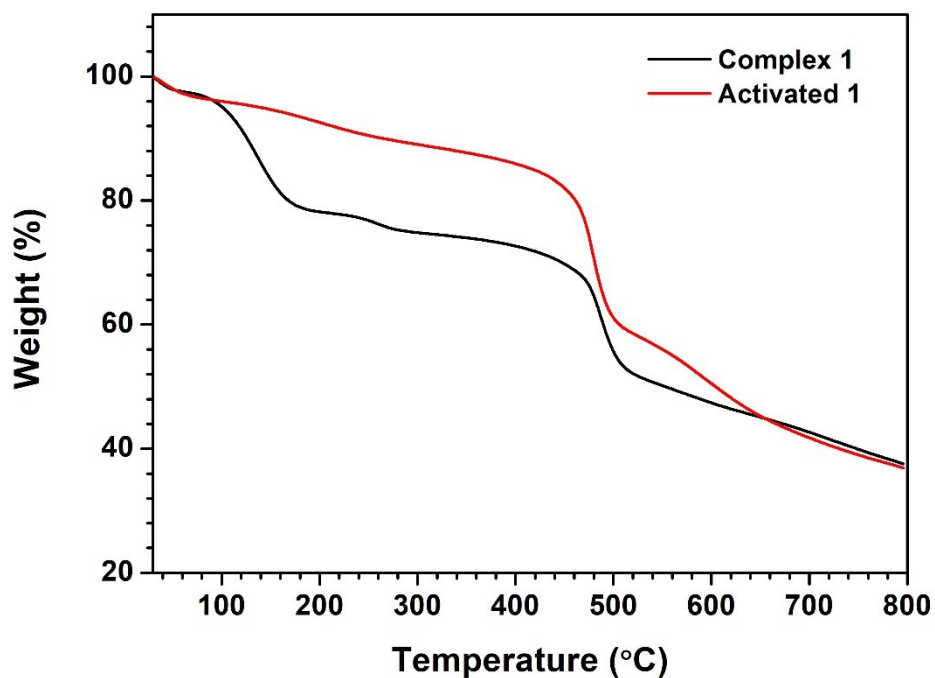


Fig. S3. Thermogravimetric (TG) analyses of complex **1** and activated **1**.

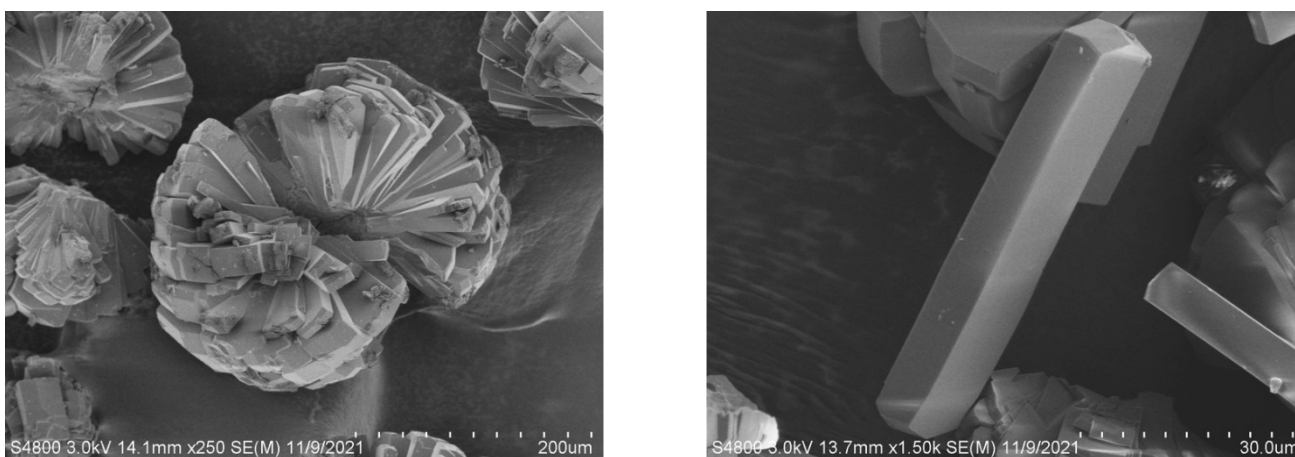


Fig. S4. The FESEM images of the complex **1**.

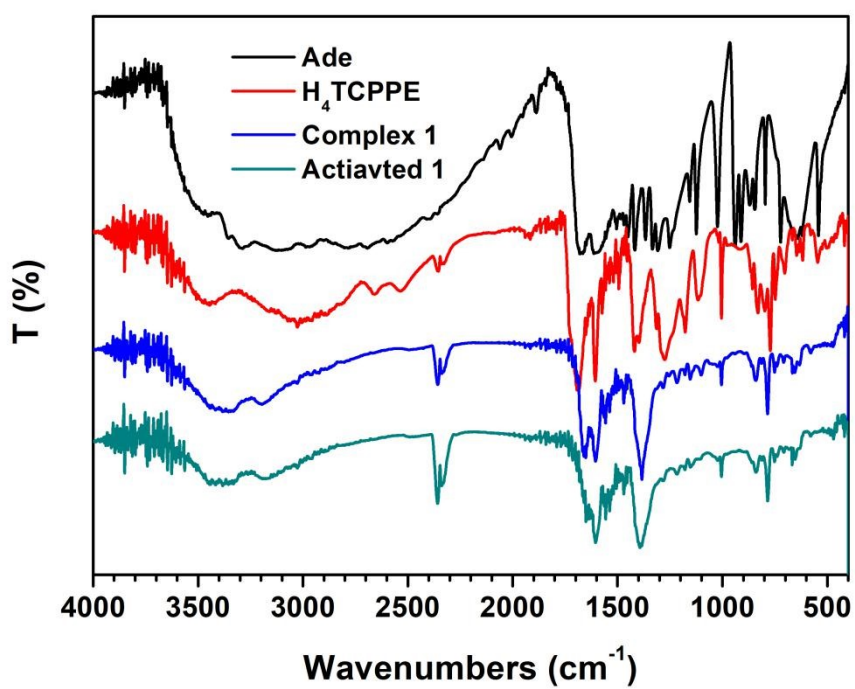


Fig. S5. FTIR spectra of Ade (black), H₄TCPPE (red), complex **1** (blue) and activated **1** (green).

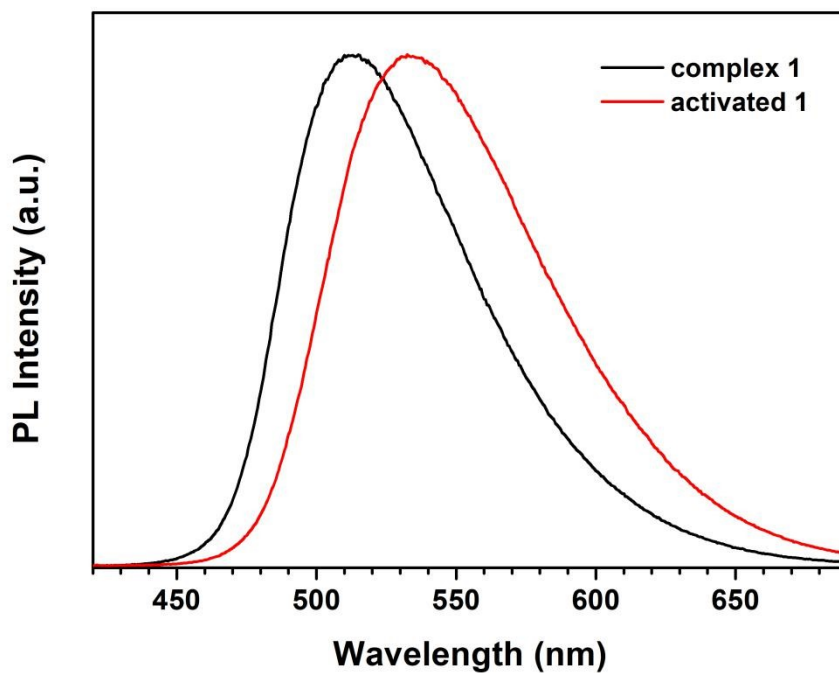


Fig. S6. Solid-state PL spectra of complex **1** and activated **1**.

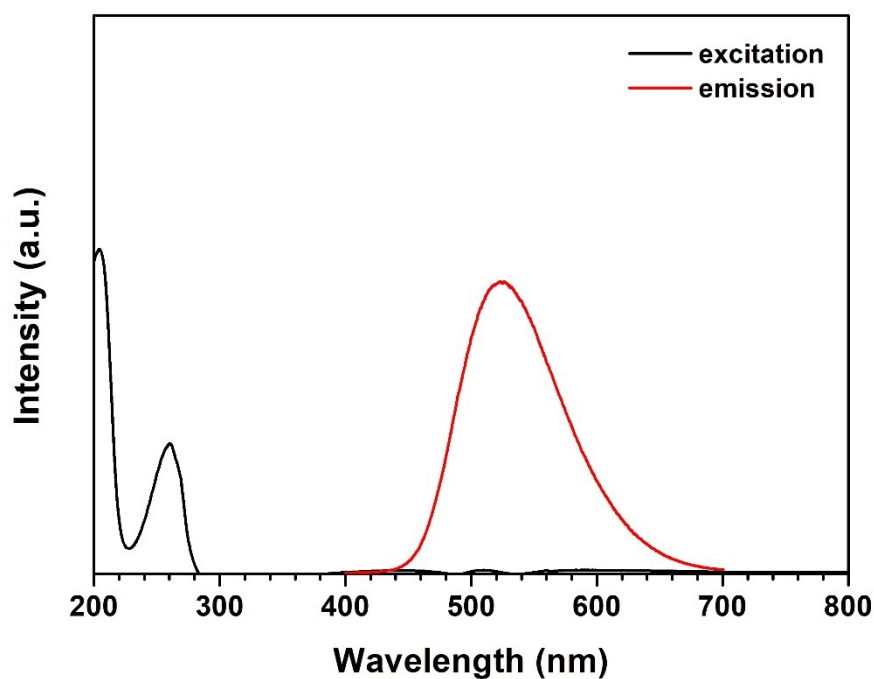


Fig. S7. Spectral overlap between the excitation and emission spectra of activated **1** aqueous suspension.

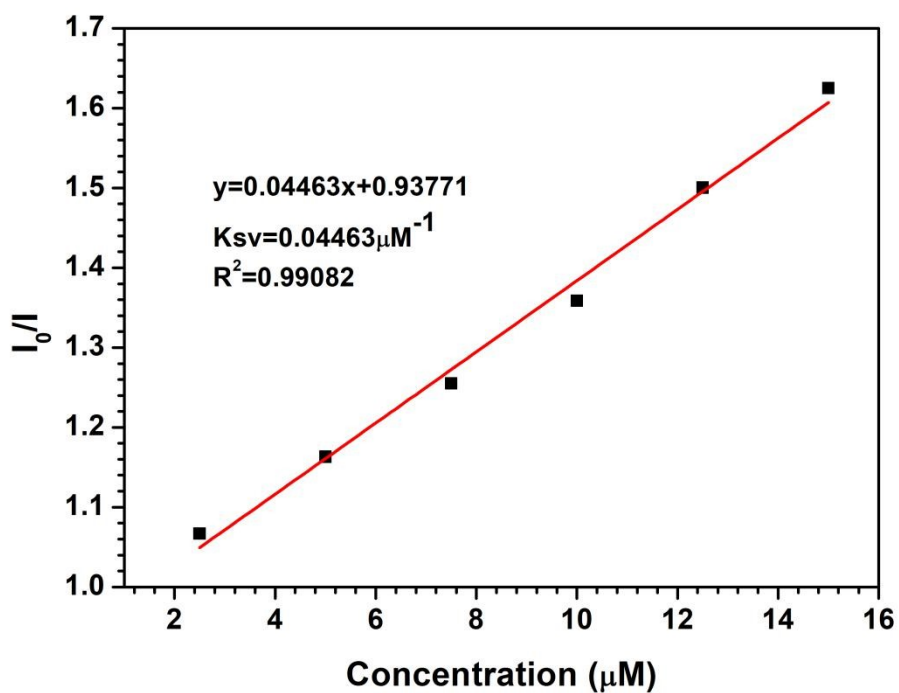
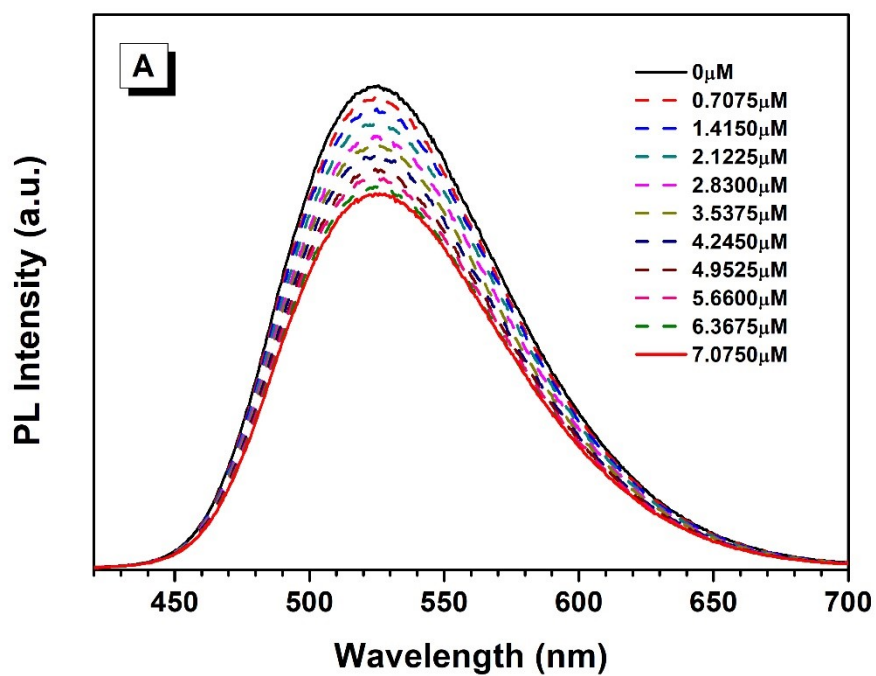


Fig. S8. The fitting plot of the I_0/I of activated **1** with the increasing concentration of L-Nph at low concentration range.



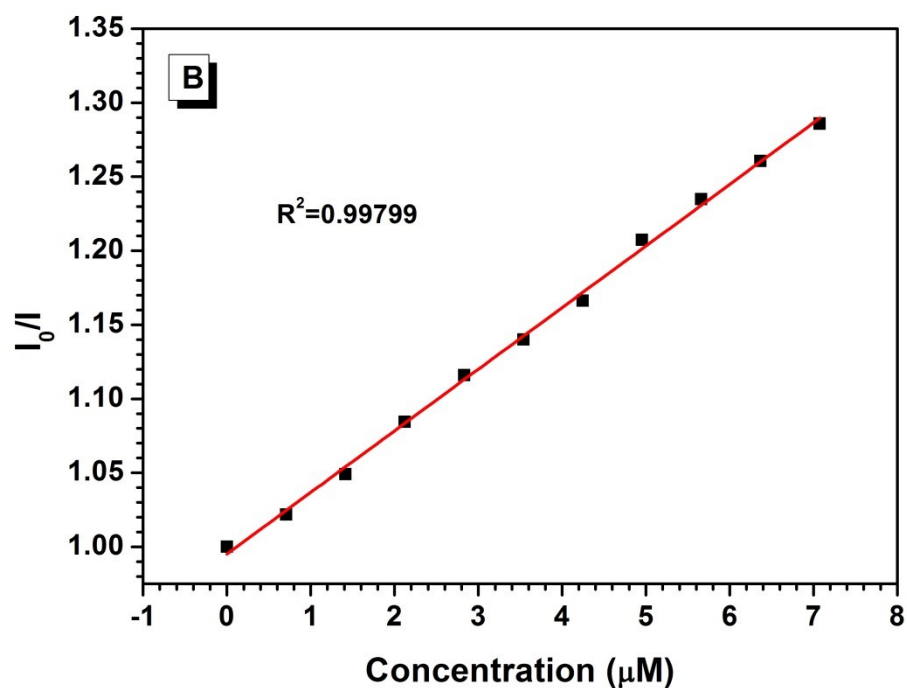
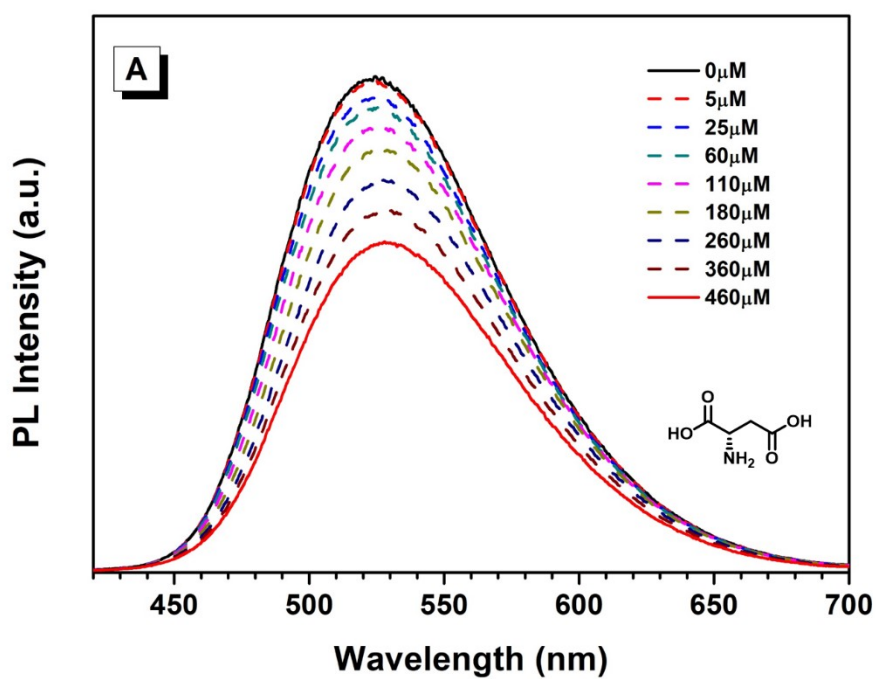
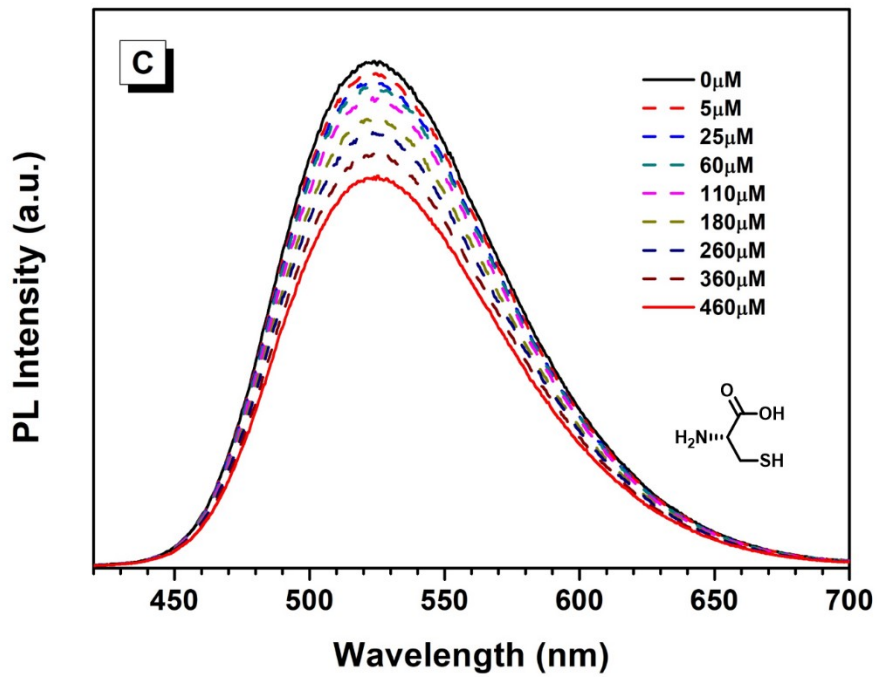
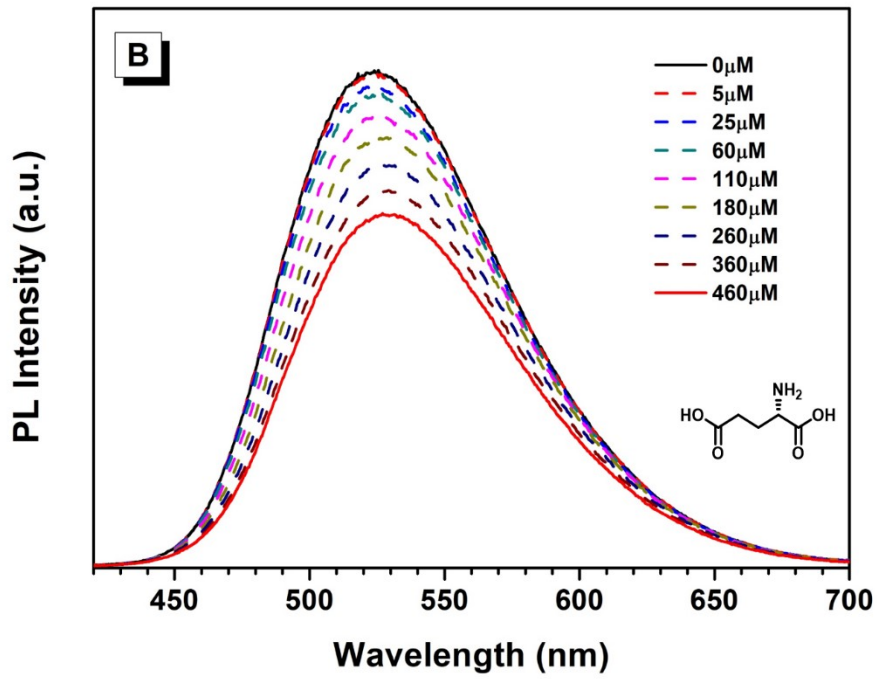
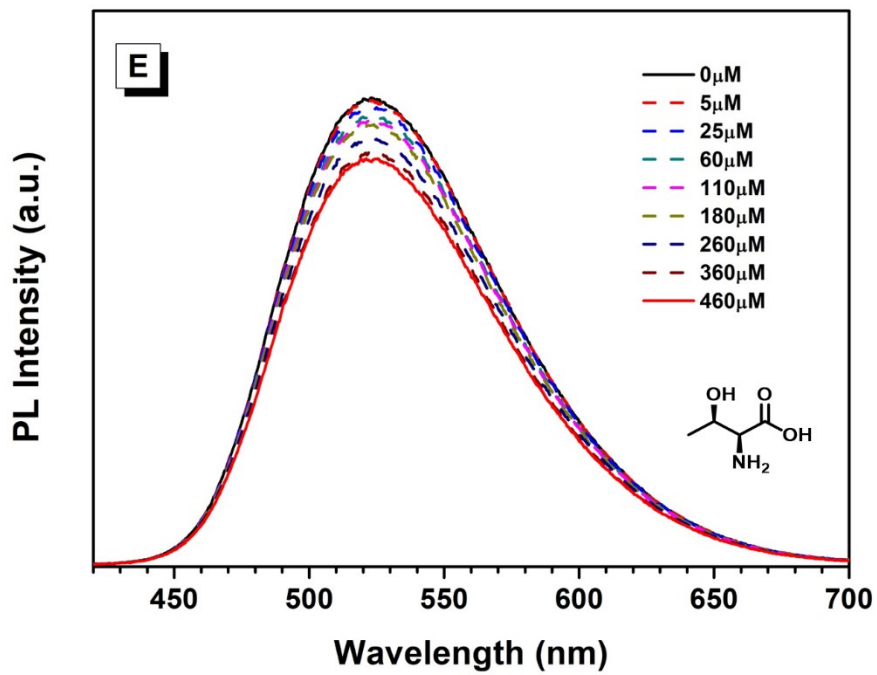
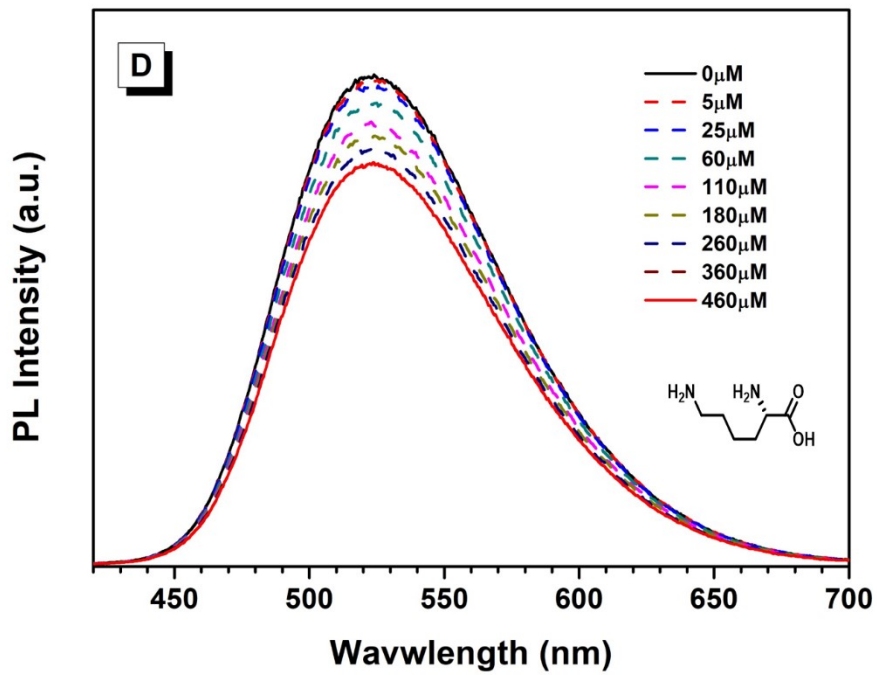
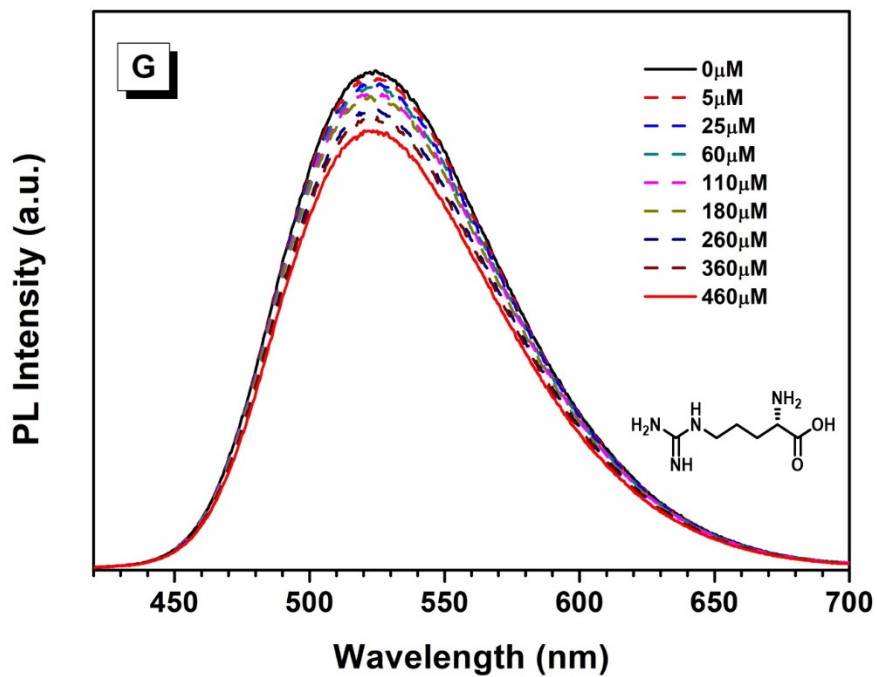
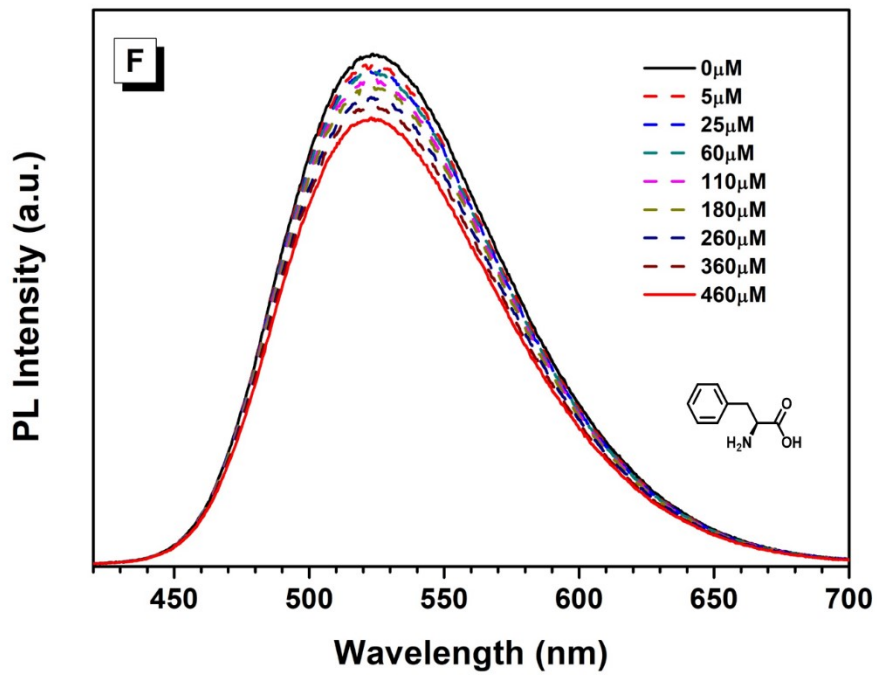


Fig. S9. (A) Emission spectra of activated **1** suspension upon addition of L-Nph aqueous solution (0.283 mM). (B) The fitting plot of the I_0/I of activated **1** suspension with the increasing concentration of L-Nph at low concentration range.









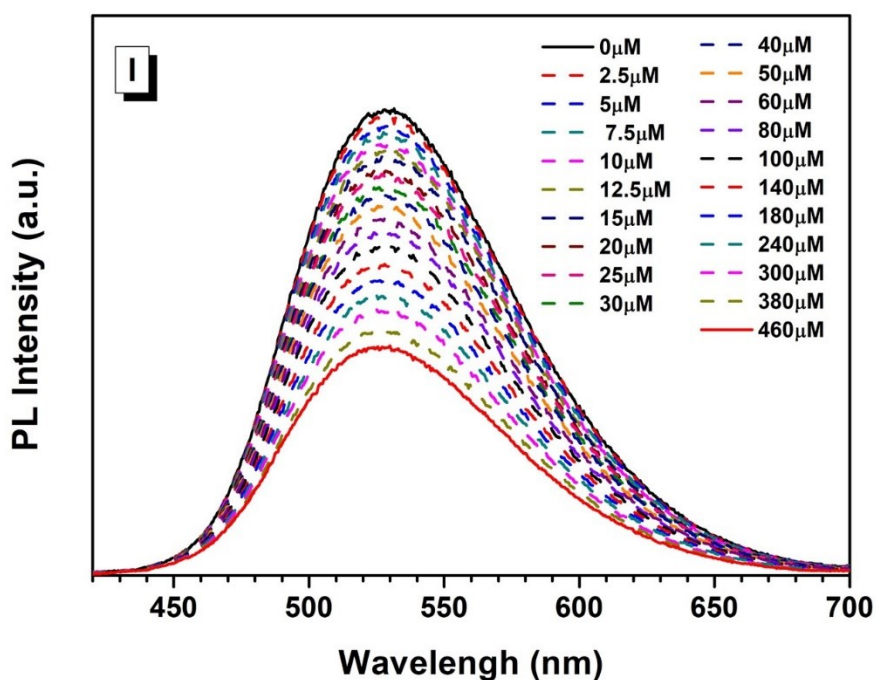
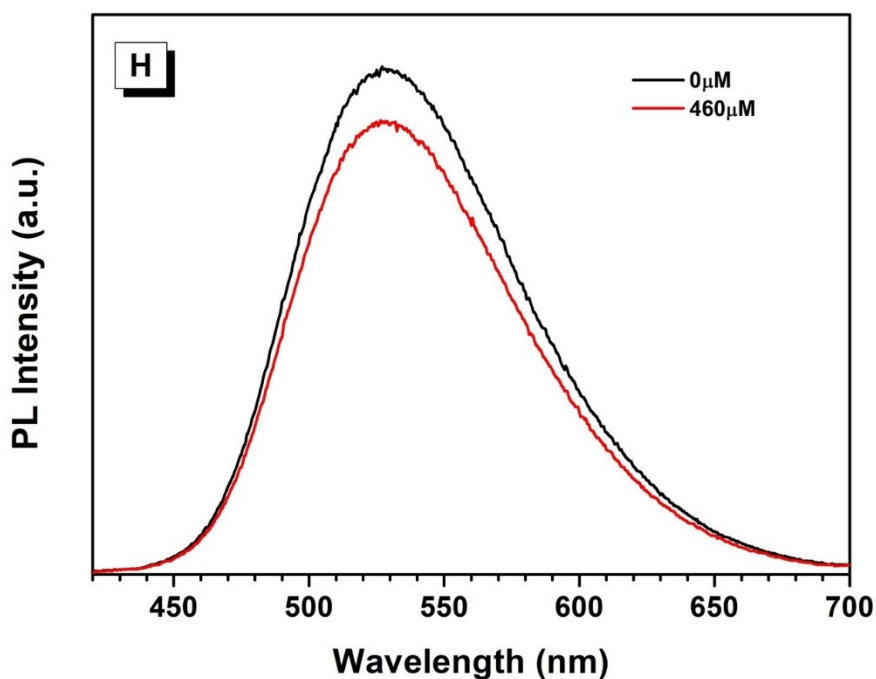


Fig. S10. Emission spectra of activated **1** aqueous suspension upon addition of different amino acids of L-Asp (A), L-Glu (B), L-Cys (C), L-Lys (D), L-Thr (E), L-Phe(F) and L-Arg (G) aqueous solution (2 mM). (H) Emission spectra of activated **1** aqueous suspension upon addition of 460 μL water. (I) Emission spectra of activated **1** aqueous suspension upon addition of a mixed aqueous solution of all amino acids.

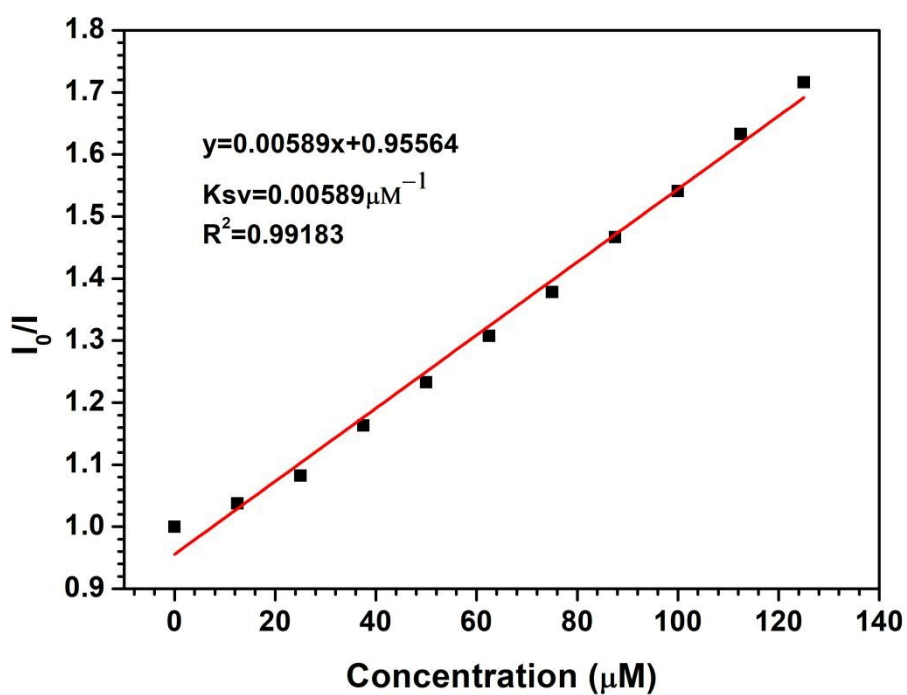
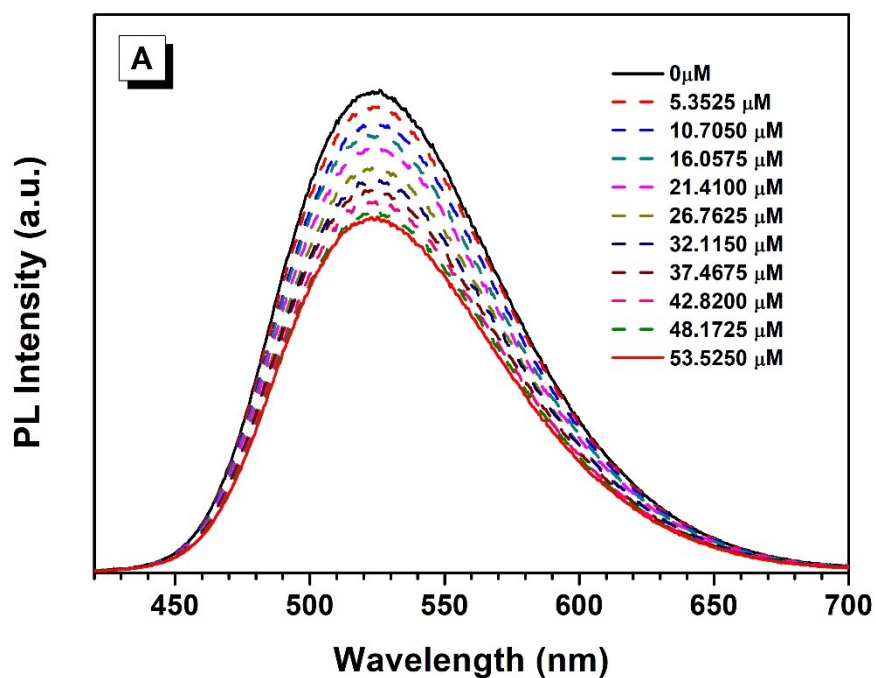


Fig. S11. The fitting plot of the I_0/I of activated **1** with the increasing concentration of D-Nga at low concentration range.



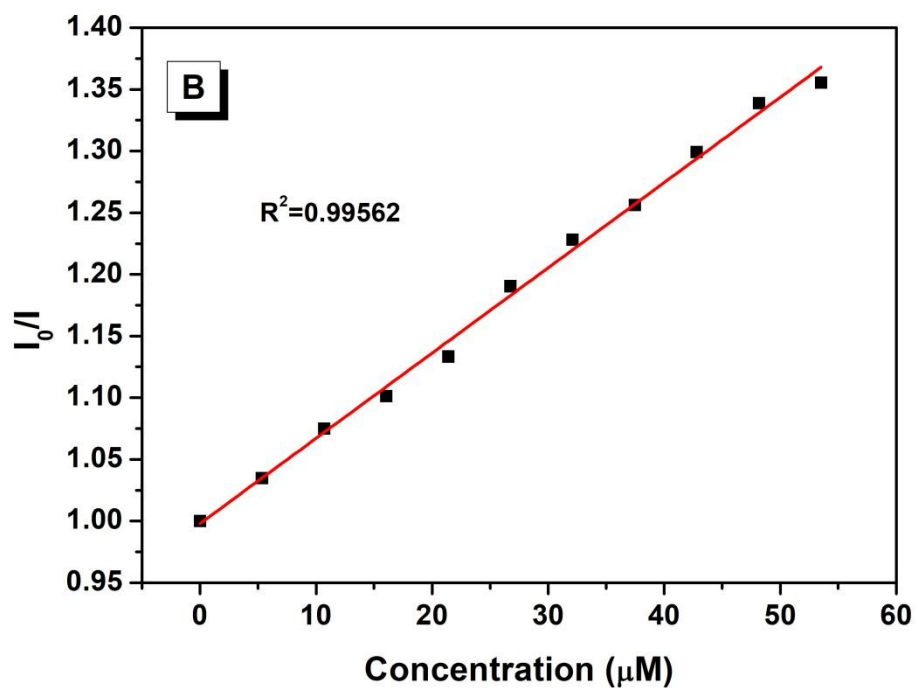
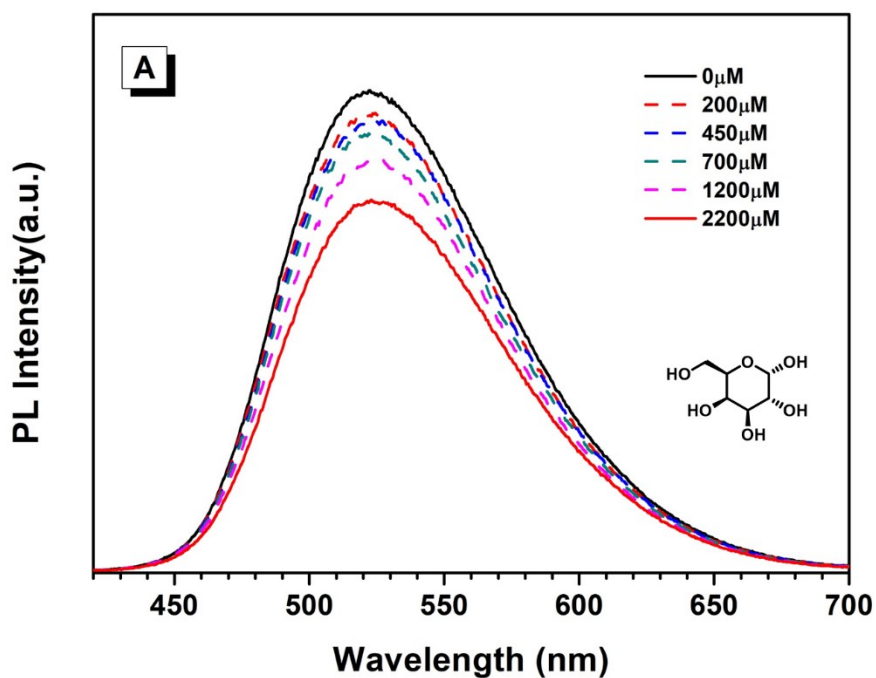
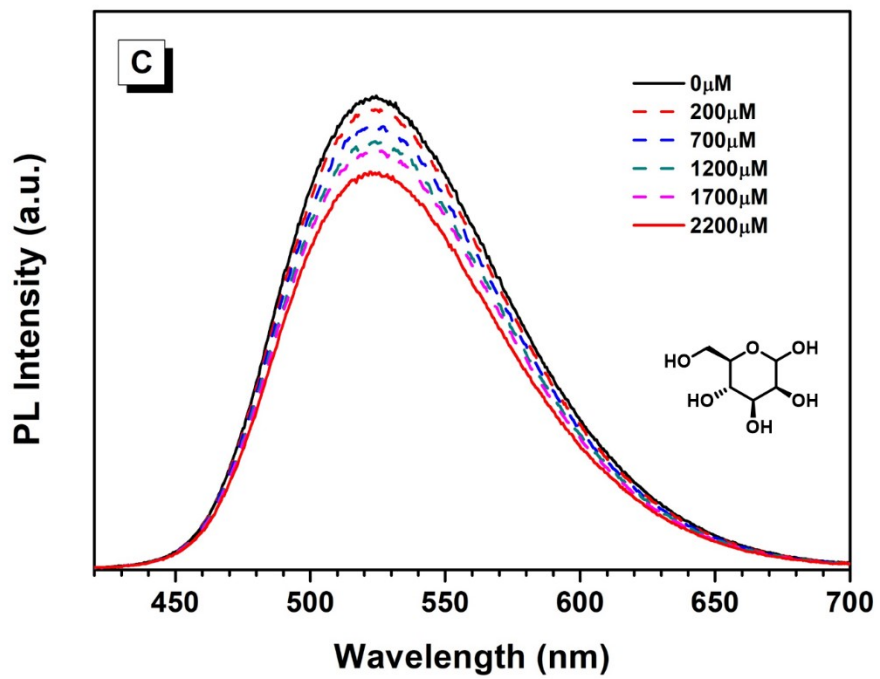
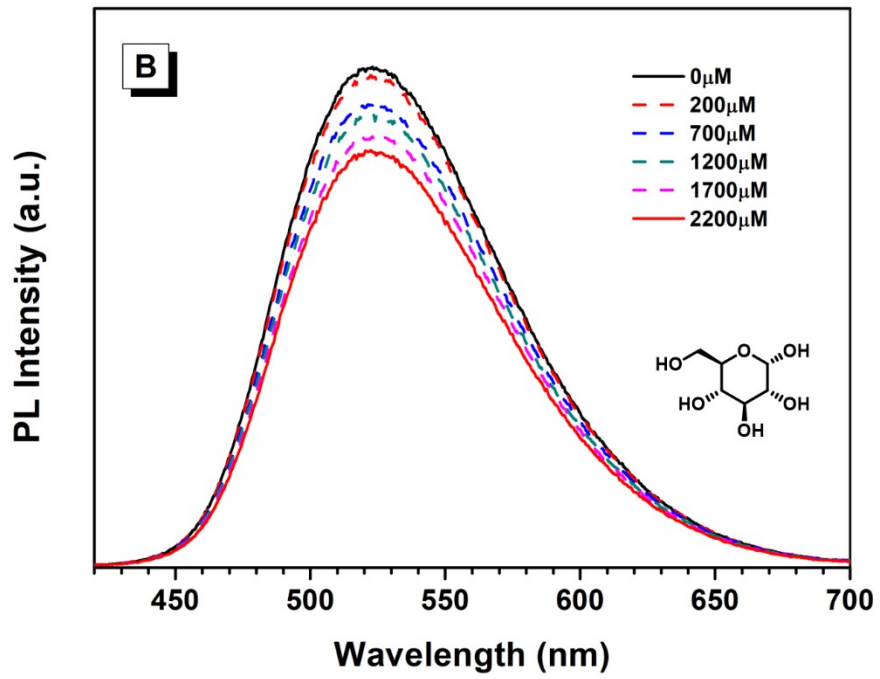
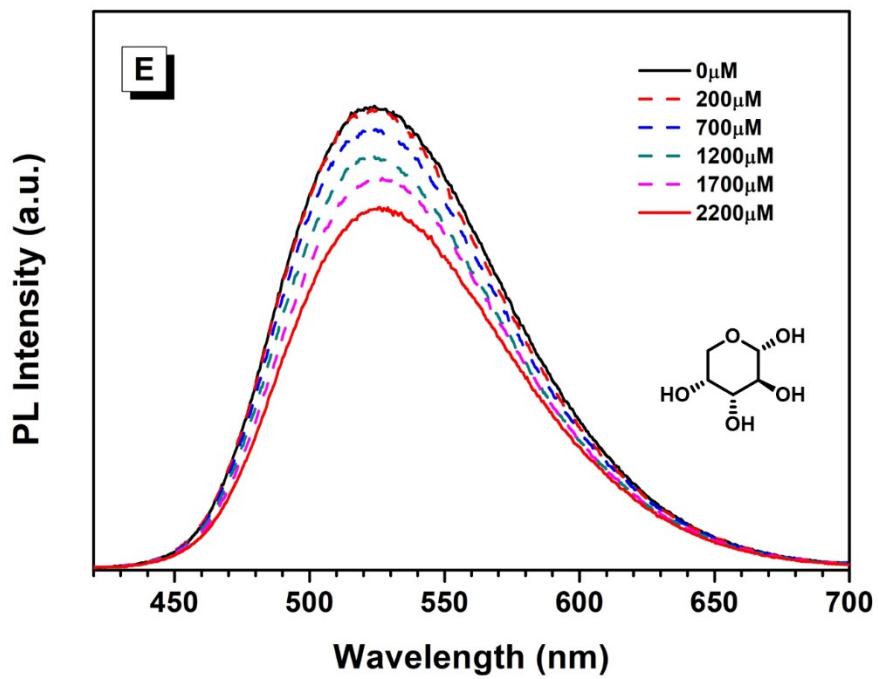
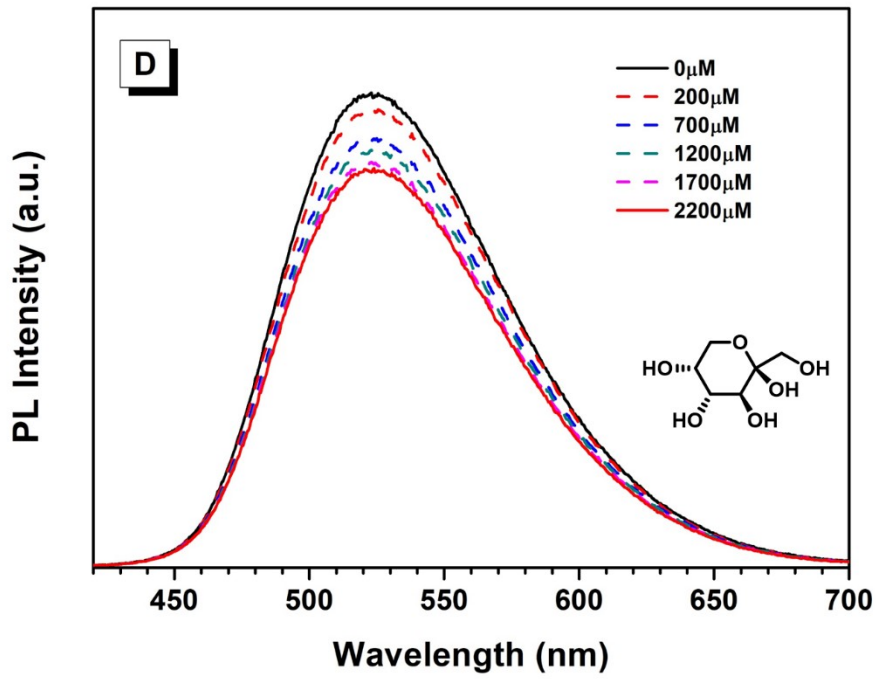
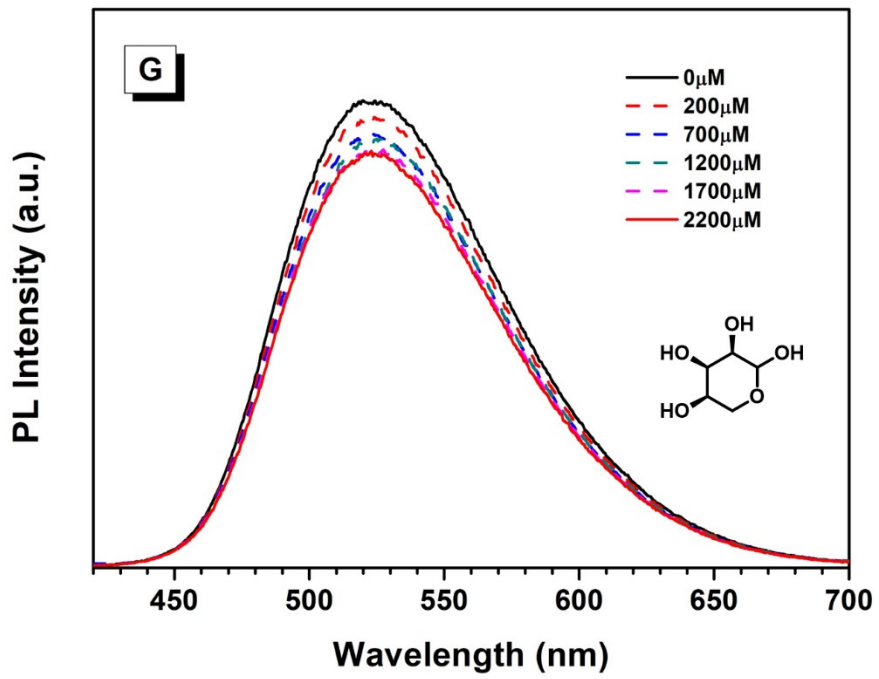
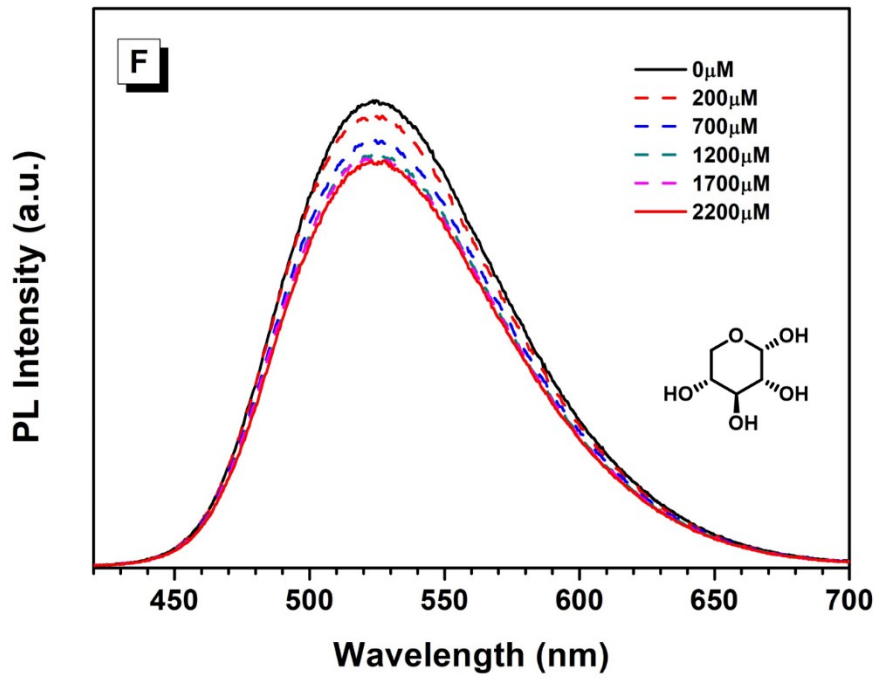


Fig. S12. (A) Emission spectra of activated **1** suspension upon addition of D-Nga aqueous solution (2.141 mM). (B) The fitting plot of the I_0/I of activated **1** suspension with the increasing concentration of D-Nga at low concentration range.









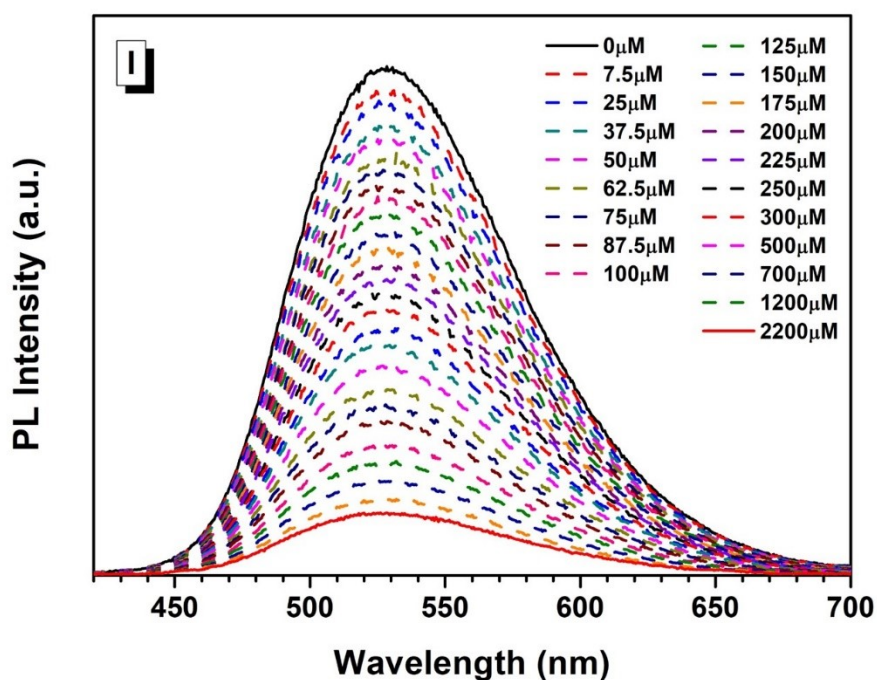
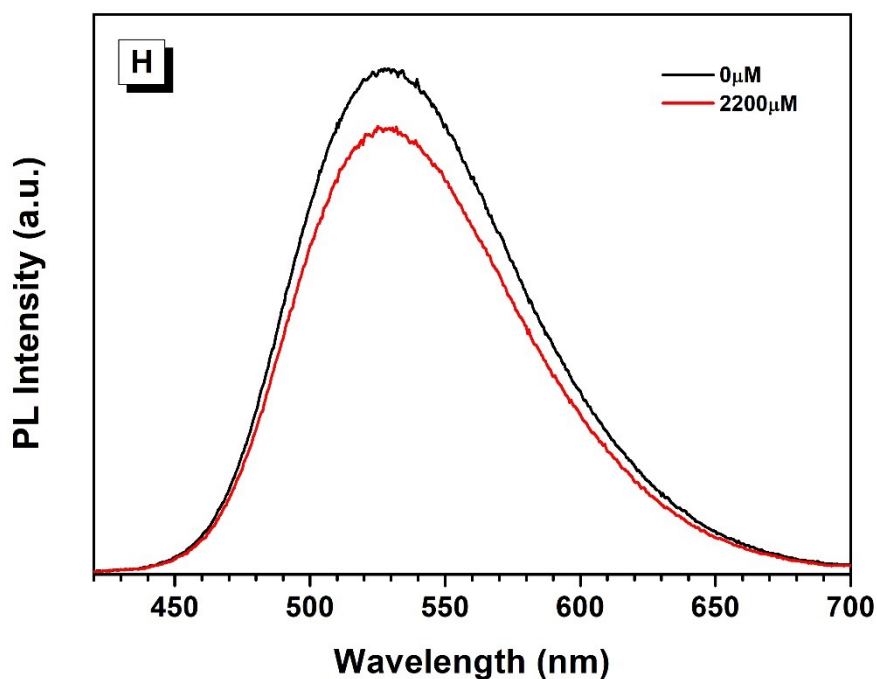


Fig. S13. Emission spectra of activated **1** aqueous suspension upon addition of different monosaccharide of D-Gal (A), D-Glu (B), D-Man (C), D-Fru (D), D-Ara (E), D-Xyl (F) and D-Rib (G) aqueous solution (10 mM). (H) Emission spectra of activated **1** aqueous suspension upon addition of 440 μL water. (I) Emission spectra of activated **1** aqueous suspension upon addition of a mixed aqueous solution of all monosaccharide.

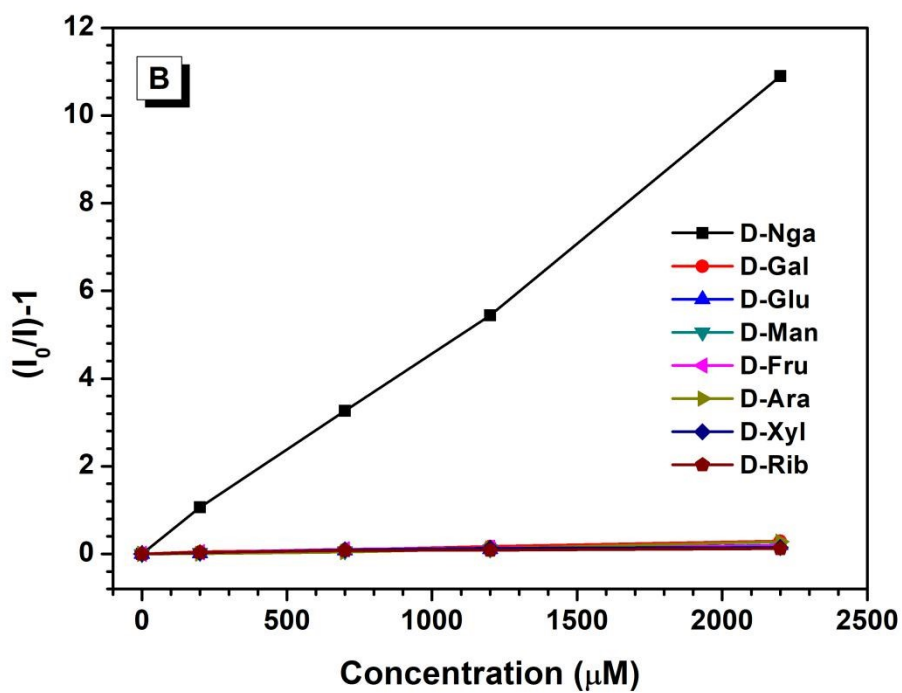
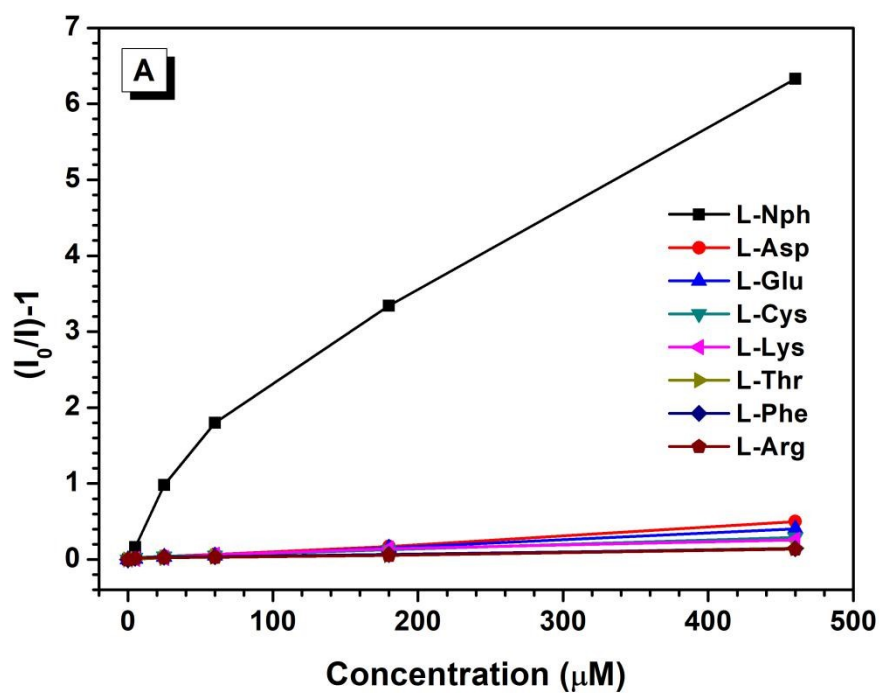


Fig. S14. Stern-Volmer (SV) plots for amino acids (A) and monosaccharides (B) aqueous solution.

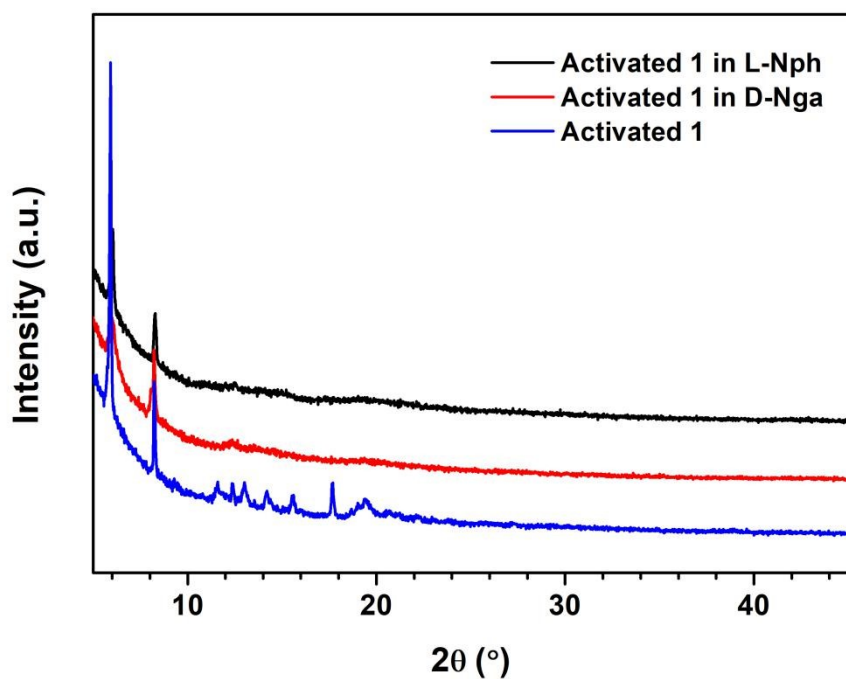
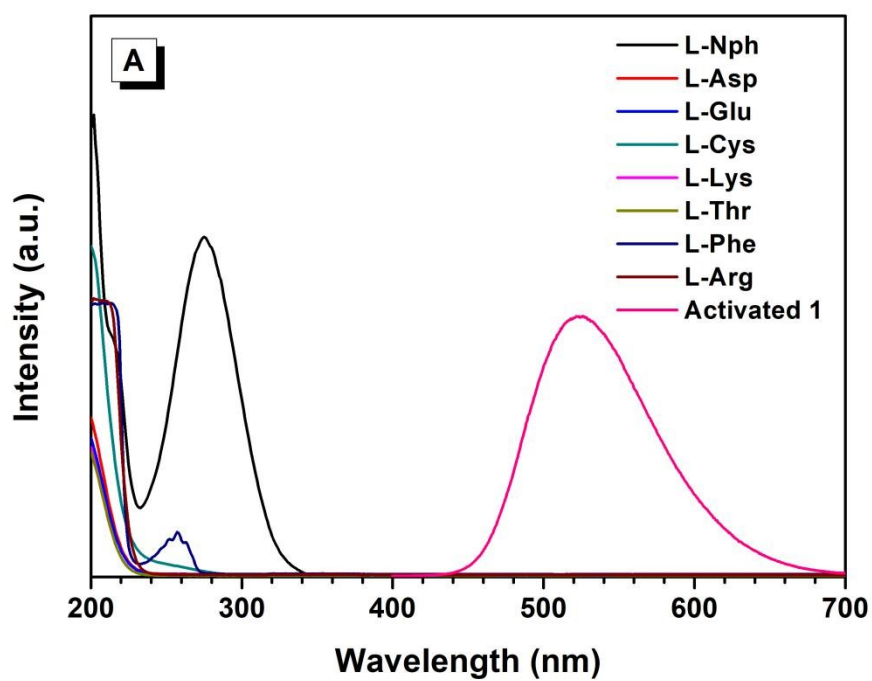


Fig. S15. PXRD patterns of activated **1** (blue) and activated **1** after being soaked in L-Nph (black) and D-Nga (red), respectively.



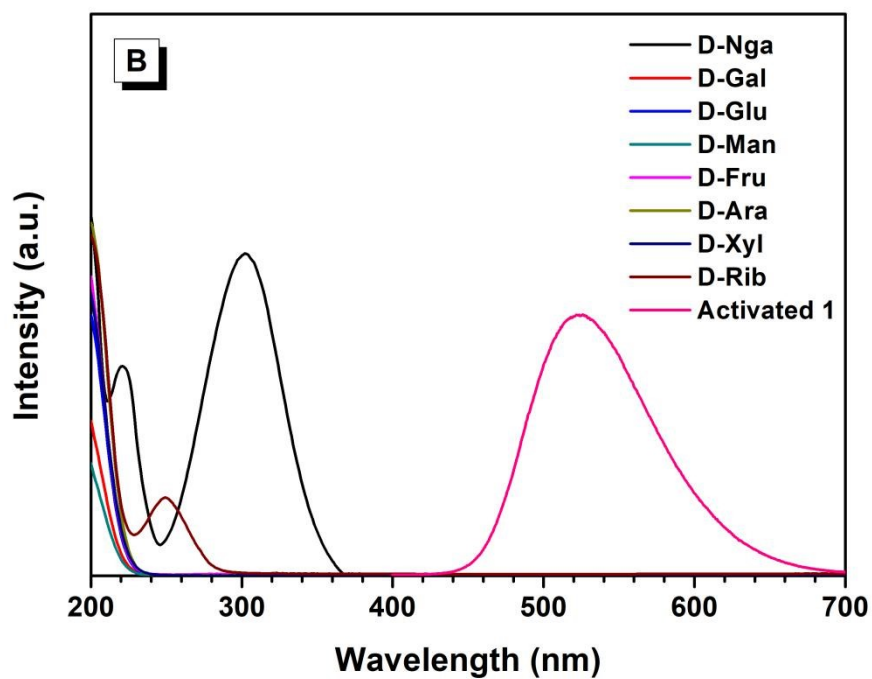
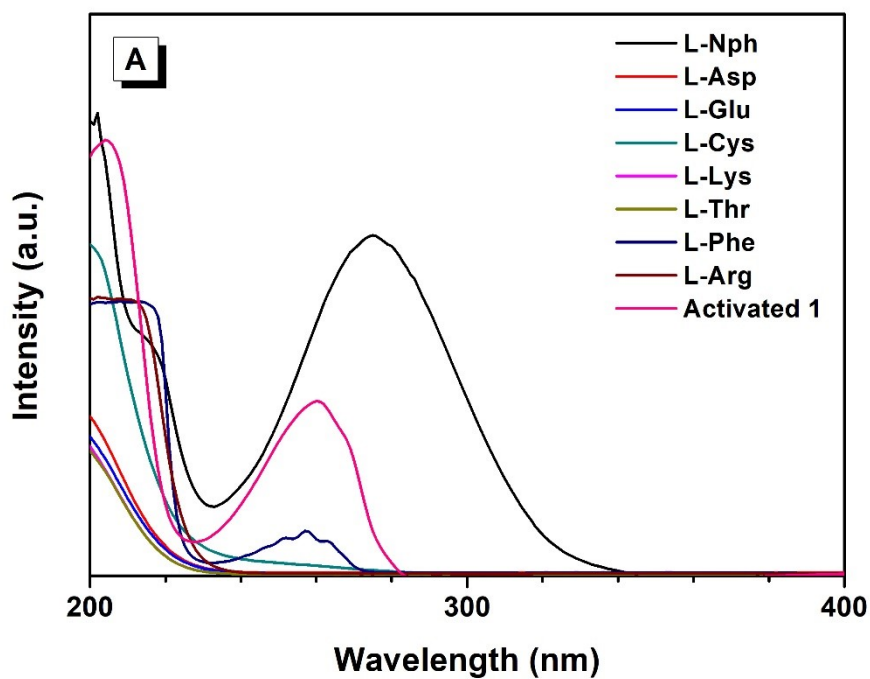


Fig. S16. Spectral overlap between the UV-vis spectra of amino acids (A) and monosaccharides (B) aqueous solution and the emission spectrum of activated **1** aqueous suspension.



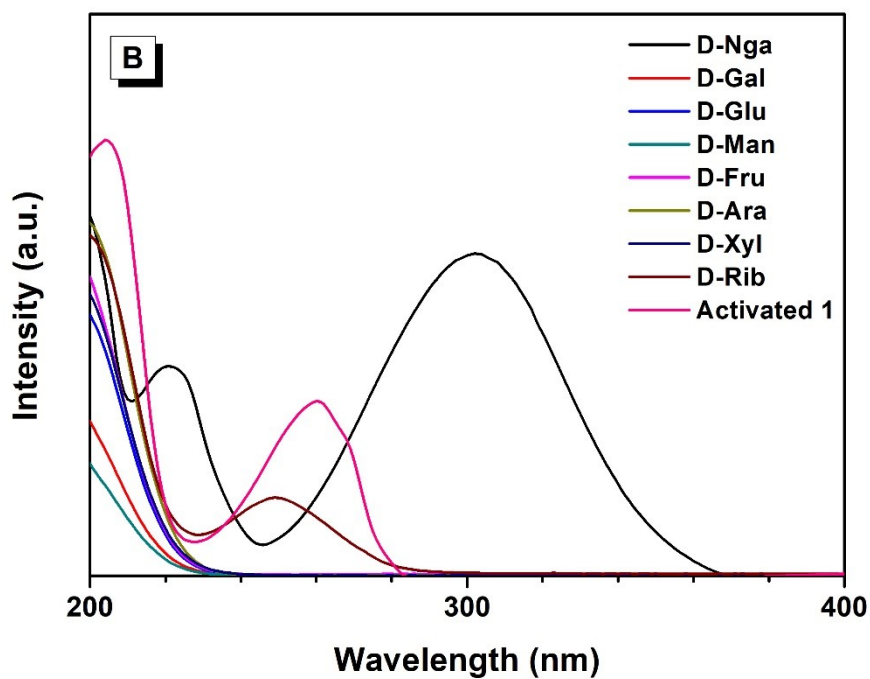


Fig. S17. Spectral overlap between the UV-vis spectra of amino acids (A) and monosaccharides (B) aqueous solution and the UV-vis spectra of activated **1** aqueous suspension.